

Subgraph nomination: Query by Example Subgraph Retrieval in Networks

Al-Fahad M. Al-Qadhi¹, Carey E. Priebe²,
Hayden S. Helm³, Vince Lyzinski¹

¹ University of Maryland, College Park, Department of Mathematics

² Johns Hopkins University, Department of Applied Mathematics and Statistics

³ Johns Hopkins University, Center for Imaging Science

February 1, 2021

Abstract

This paper introduces the subgraph nomination inference task, in which example subgraphs of interest are used to query a network for similarly interesting subgraphs. This type of problem appears time and again in real world problems connected to, for example, user recommendation systems and structural retrieval tasks in social and biological/connectomic networks. We formally define the subgraph nomination framework with an emphasis on the notion of a user-in-the-loop in the subgraph nomination pipeline. In this setting, a user can provide additional post-nomination light supervision that can be incorporated into the retrieval task. After introducing and formalizing the retrieval task, we examine the nuanced effect that user-supervision can have on performance, both analytically and across real and simulated data examples.

1 Introduction

This paper introduces the *subgraph nomination* inference task, in which example subgraphs of interest are used to query a network for similarly interesting subgraphs. Stated succinctly, the subgraph nomination problem is as follows: given a subgraph or subgraphs of interest in a network G_1 , we seek to find heretofore unknown subgraphs of interest in G_1 or in a second network G_2 . The subgraph nomination problem can be viewed as an amalgam of the problems of noisy subgraph detection [20, 5, 24, 29, 38] and vertex nomination [27, 7, 11, 25], in which our task is to produce a rank-list of candidate subgraphs, with (ideally) unknown subgraphs of interest concentrating at the top of the rank list. While seemingly simple on its surface, subgraph nomination necessarily entails the often non-trivial combination of subgraph detection (i.e., we have to find candidate subgraphs to rank) and multiple graph comparison methodologies (i.e., we have to rank the candidate subgraphs).

Subgraph detection—here, producing candidate subgraphs of interest from G_1 or G_2 —is an active area of research in machine learning and pattern recognition, and encompasses

both the famous subgraph isomorphism problem (see, for example, [2, 37, 8, 41]) as well as numerous noisy subgraph detection routines. In subgraph nomination, subgraph detection is further complicated by the generality of the (topological) features that define the training subgraphs as “interesting.” In particular, it may be the case that the query set encompasses multiple different interesting templates [29, 20] or motifs-of-interest [28, 26], each delineating an activity or structure of interest in the network. Moreover, the templates of interesting subgraphs need not be manifestly similar to each other. The notion of *similarity* across subgraphs will be formalized via a subgraph dissimilarity mapping Δ , and a subgraph nomination scheme can (loosely) be considered as an estimate of the subgraph structure of g_2 combined with a dissimilarity Δ used to rank the subgraphs (see Def. 2.5). If \mathfrak{S}_G represents the collection of all subgraphs of a network G , then in the single-graph setting

$$\Delta : \mathfrak{S}_{G_1} \times \mathfrak{S}_{G_1} \rightarrow [0, 1],$$

and in the pair of graphs setting

$$\Delta : \mathfrak{S}_{G_1} \times \mathfrak{S}_{G_2} \rightarrow [0, 1],$$

with smaller values indicating more similar subgraphs. We comment here that although the two graph setting will be our focus moving forward, this naturally lifts to the single graph setting by considering the two graphs to nominate across as parts of a partition of a larger network.

Large values of Δ indicate that the subgraphs are highly dissimilar according to Δ , and candidate subgraphs are defined as interesting if they are sufficiently similar (i.e., insufficiently dissimilar) to *any* subgraph in the training sample. Choosing an appropriate Δ from which to construct the subgraph rankings is of primary import, and adaptive methods (similar to those in the learning-to-rank problem in the information retrieval literature [23, 18]) can be considered to learn Δ from the training subgraphs of interest. While estimating an optimal Δ is central in this problem framework, we do not derive formal procedures for estimating Δ in this paper. Instead, we choose to focus on the effect of user-in-the-loop supervision across a variety of possible Δ choices, where the user is modeled as additional light supervision that can be used to refine the output of a subgraph nomination routine.

As a motivating example for our focus on studying the effects of a user-in-the-loop, we consider the problem of detecting and nominating particular brain regions of interest across the hemispheres of a human connectome from the BNU1 dataset [43] downloaded from <https://neurodata.io/mri/>. In this setting, subgraph nomination can be used as a tool to better understand (and detect) the structural similarity between brain regions across hemispheres. To this end, we consider a region (or regions) of interest in the left hemisphere, and there might be multiple subgraphs in the right hemisphere that match (according to Δ) well to the training data. Moreover, the most similar region of interest in the right hemisphere (i.e., the Δ -optimal subgraph of the right hemisphere) may vary dramatically depending on the Δ used (see, for example, Figure 7 in [38]), and the optimal region may not significantly overlap with a true latent region of interest in the left hemisphere. In this case, even a sensible ranking scheme would be potentially unable to correctly retrieve the desired region of interest in the right hemisphere (even if the proper subgraph was identified). In this case, we can naturally employ the help of a user-in-the-loop [3], who, given a vertex, can decide whether it is interesting/part of an interesting subgraph to help refine our ranking.

The subgraph nomination framework we present in this paper is both general enough to include the operationally significant effect of a user-in-the-loop and principled enough to theoretically analyze nomination schemes. After discussing preliminaries and presenting the problem framework, we demonstrate multiple pathologies to highlight the power of the subsequent theory as a predictive tool of the efficacy of the user in general situations. In particular, we show that a user can improve the performance over a scheme that achieves the Bayes optimal rate sans user-in-the-loop, even in the presence of potential user-error. This result is similar to results in the classification literature when given noisy training labels [16, 30]. We further show that, given noisily recovered subgraphs, including information from an oracle user can deteriorate performance due to the noise within the subgraph detection routines.

Notation: For a positive integer n , we will denote $[n] := \{1, 2, 3, \dots, n\}$; J_n to the $n \times n$ matrix of all 1's; \mathcal{G}_n to be the set of labeled n -vertex graphs; for $G \in \mathcal{G}_n$, and $W \subset V(G)$, we let $G[W]$ denote the induced subgraph of G on W .

2 Introduction and Background

In subgraph nomination, our task is as follows: given a subgraph or subgraphs of interest in a network G_1 , we seek to find heretofore unknown subgraphs of interest in a second network G_2 . Our approach to subgraph nomination proceeds by

1. Partitioning the vertices in G_2 into candidate subgraphs (note that the choice of non-overlapping candidate subgraphs is merely a theoretical/notational convenience, and in practice, the subgraphs to be ranked can have overlap);
2. Ordering the candidate subgraphs in G_2 into a rank list with the unknown subgraphs of interest ideally concentrating at the top of the rank list.

Subgraph nomination is a natural extension of vertex nomination (VN) [27, 7, 39, 12, 25, 1], and we will begin by providing a brief background on recent developments in VN, as this will provide useful context for our later novel formulation of subgraph nomination.

2.1 Vertex Nomination

Semi-supervised querying of large graphs and databases is a common graph inference task. For example, in a graph database with multiple features, one may be given a collection of book names all with the common *latent* feature “Horror Fiction Best Sellers,” and the goal would be to query the database for more titles that fit this description; see, for example, the work in [4, 34]. Learning this unifying feature from the query set is a challenging problem unto itself [35], especially in settings where the features that define interestingness are nuanced or multi-faceted.

While we can interpret such a problem as a vertex classification problem where vertices are either labeled interesting or not, in the presence of very large networks with large class imbalance between interesting and non-interesting vertices, there is often limited training data and limited user resources for verifying returned results. In this setting, an information

retrieval (IR) framework may be more appropriate, wherein unlabeled vertices would be ordered in a rank list based on how interesting they are deemed to be. This inference task is synonymous with *vertex nomination* (or personal recommender systems on graphs).

In [32, 25, 1, 21], the vertex nomination problem is defined as follows. Given vertices of interest $V^* \subset V(G_1)$ in a network G_1 , and corresponding unknown vertices of interest $U^* \subset V(G_2)$ in a second network G_2 (whose identities are hidden to the user), use G_1, G_2, V^* to rank the vertices in G_2 into a nomination list, with vertices in U^* concentrating at the top of the nomination list. In its initial formulation [7, 27, 12, 42], the feature that defined vertices as interesting was membership in a community of interest, and the community memberships of vertices in V^* were used to nominate the vertices in G_1 (no second network was introduced, or $G_2 = G_1 \setminus \{V^*\}$) with unknown community memberships. Subsequent work [34, 35, 32, 25] sought to generalize the features that defined vertices as interesting beyond simple community membership, and lifted the vertex nomination problem to the two graph setting.

In order to allow for a broadly general class of networks to be considered, the general vertex nomination problem framework of [1, 25] referenced above is situated in the context of nominatable distributions, a broad class of random graph distributions defined in [1]. Within this broad class of models, the concepts of Bayes optimality and consistency were developed in [25, 1] and the important result that universally consistent VN schemes do not exist is proven in [25]. These results were leveraged in [1] to develop an probabilistic adversarial contamination model in the context of VN as well as regularization schemes to counter the adversary. The results of [25, 1] were further extended to the richly featured network setting in [21], in which the (potentially) complementary roles of features and network structure are explored in the VN task.

Beyond the development of novel VN algorithms [42], one of the key aspects of the recent theoretical developments in VN is the notion that vertex labels in g_2 are uninformative in the ranking scheme, which is sensible if we are mirroring setting in which the vertex labels do not aid in the delineation between interesting and uninteresting vertices. In subgraph nomination, the uninformative nature of the labels can be accounted for in the dissimilarity Δ (see Eq. 1). Note that while similar consistency results to those in VN can be derived in the setting of subgraph nomination, we do not focus on that here. Rather we will focus on the role of users-in-the-loop in the subgraph nomination framework.

2.2 Hierarchical Subgraph Models

We will use \mathcal{G}_n to denote the set of n -vertex labeled graphs on a common vertex set $V = V_n$. Given the (informal) explanation of the motivating task in subgraph nomination—given light supervision, partition a graph into subgraphs and rank the subgraphs based on how interesting they are judged to be—hierarchical network models are a natural setting for initially formalizing the subgraph nomination inference task. Hierarchical models have seen a surge in popularity in the network literature (see, for example, [36, 6, 31, 33, 26, 22]) and naturally allow for multiple layers of structure to be simultaneously modeled in a network, allowing us to imbue a graph G with subgraph structures of a desired form or motif-type. We begin with our definition of a hierarchical network as a network together with a *Network Hierarchical Function*.

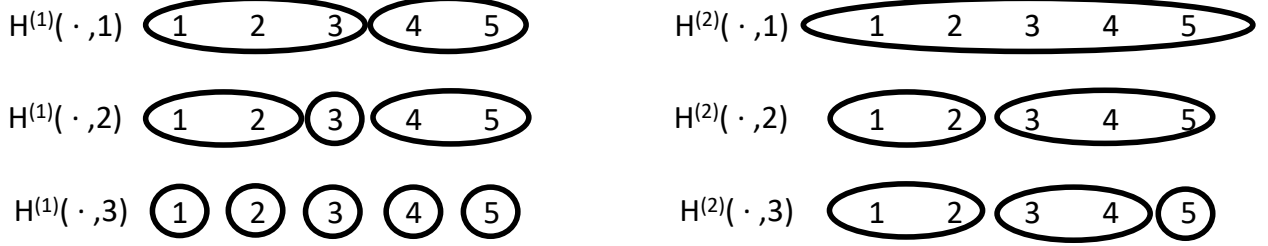


Figure 1: An example of two 3-Level network hierarchical functions of [5], $H^{(1)}$ and $H^{(2)}$. Note the nestedness, and the fact that we do not require the top level to be a single cluster nor the bottom layer to be $n = 5$ clusters.

Definition 2.1. Let $g = (V, E) \in \mathcal{G}_n$, and for each $i \in \mathbb{Z} > 0$ let $[i] = \{1, 2, \dots, i\}$. Let $k \leq n$. A function

$$H = H_k : V \times [k] \longrightarrow [n]$$

is a k -level Network Hierarchical Function of $[n]$ if

- i. For each $i \in [k]$, $H(\cdot, i)$ represents a partition of the vertices of V into $n_i := n_i^{(H)}$ nonempty parts (so that $\max_v H(v, i) = n_i$). These n_i satisfy $1 \leq n_1 \leq n_2 \leq \dots \leq n_k \leq n$. The signature of H is defined to be the vector $\vec{n} = (n_1, n_2, \dots, n_k)$. Note that by considering appending 0's onto the end of \vec{n} as needed to make it length n , we can consider the signature of an n vertex hierarchical graph to be a length n vector.
- ii. $H(v_1, j) = H(v_2, j)$ only if $H(v_1, i) = H(v_2, i)$ for all $i \leq j$; i.e., the partition is nested.

For an example of network hierarchical functions, see Figure 1. A graph $g \in \mathcal{G}_n$ together with a Network Hierarchical Function H_k of $[n]$ is a k -level Hierarchical Graph. For $k \leq n$, we denote

$$\mathcal{H}_{k,n} = \{H_k \mid H_k \text{ is a } k\text{-level Network Hierarchical Function of } [n]\},$$

and we define

$$\mathcal{HG}_n := \{(g, H) \mid g \in \mathcal{G}_n, \text{ and } H \in \cup_{k=1}^n \mathcal{H}_{k,n}\}$$

to be the set of all Hierarchical graphs of order n .

Letting $k \leq n$, let $H \in \mathcal{H}_{k,n}$. For each $i \in [k]$ and $j \in [n_i]$, we define the sets

$$B_j^i = \{v \in V(g) \mid H(v, i) = j\}$$

to be the set of vertices in the j -th part of the i -th level of the hierarchy;

$$B_{(j)}^{i-1} = \{v \in V(G) \mid \text{for all } v' \in B_j^i, H(v, i-1) = H(v', i-1)\}$$

to be the one-step upward merge of B_j^i in the hierarchy;

$$B^i = \{B_j^i \mid 1 < j < n_i\}$$

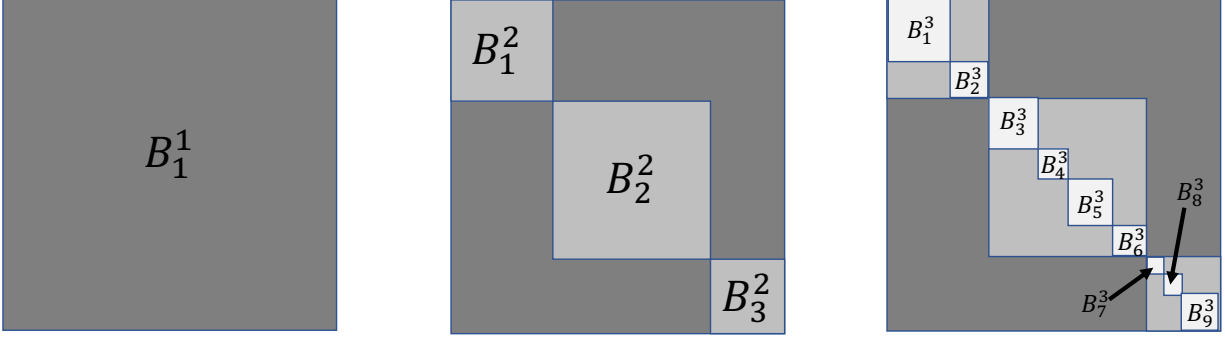


Figure 2: An example of a 3-Level hierarchical network (where the three levels are shown in the right panel, the top two levels in the middle panel, and the highest level in the left panel). The partition provided by $H(\cdot, 1)$ is in darkest grey; the partition provided by $H(\cdot, 2)$ is in medium grey; and the partition provided by $H(\cdot, 3)$ is in lightest grey.

to be the set of all parts at level i in the hierarchy; and

$$B = \{B^i : i \in [k]\}.$$

to be the set of blocks. As an example, consider the hierarchical network in Figure 2, which shows a 3-level hierarchical network, where we have (for example):

$$\begin{aligned} n_1 &= 1; n_2 = 3; n_3 = 9; \\ B_1^1 &= V = B_1^2 \cup B_2^2 \cup B_3^2; \\ B_{(3)}^2 &= B_3^3 \cup B_4^3 \cup B_5^3 \cup B_6^3; \\ B^3 &= \{B_1^3, B_2^3, B_3^3, B_4^3, B_5^3, B_6^3, B_7^3, B_8^3, B_9^3\}; \\ B &= \{B_1^1, B_1^2, B_2^2, B_3^2, B_1^3, B_2^3, B_3^3, B_4^3, B_5^3, B_6^3, B_7^3, B_8^3, B_9^3\}. \end{aligned}$$

2.2.1 Hierarchical Stochastic Blockmodels

One important example of a network distribution with hierarchical structure is the hierarchical stochastic blockmodel (HSBM) [33, 26]. Before defining the HSBM, we first define the standard stochastic blockmodel [19].

Definition 2.2. We say that an n -vertex random graph G is an instantiation of a stochastic blockmodel with parameters (n, K, Λ, π) (abbreviated $A \sim SBM(n, K, \Lambda, \pi)$) if

- i. The block membership vector $\pi \in \mathbb{R}^K$ satisfies $\pi(i) \geq 0$ for all $i \in [K]$, and $\sum_i \pi(i) = 1$;
- ii. The vertex set $V = V(G)$ is the disjoint union of K blocks $V = \mathcal{B}_1 \sqcup \mathcal{B}_2 \sqcup \dots \sqcup \mathcal{B}_K$, where each vertex $v \in V$ is independently assigned to a block according to a Multinomial $(1, \pi)$ distribution. For each vertex $v \in V(G)$, let b_v be the block that v is assigned to.
- iii. The block probability matrix $\Lambda \in [0, 1]^{K \times K}$ is a symmetric matrix. Conditional on the block assignment vector $\vec{b} = (b_v)$, for each pair of vertices $\{u, v\} \in \binom{V}{2}$,

$$\{\mathbf{1}\{u \sim_G v\}\} \stackrel{ind.}{\sim} \text{Bernoulli}(\Lambda[b_u, b_v]).$$

As in [33], we will define the HSBM recursively from the top down. In essence, the 2-level HSBM is an SBM where each block itself has an SBM structure. If further, every one of the blocks of the second level is an SBM then we have a three level HSBM, and so on. Formally, we have the following recursive definition.

Definition 2.3. *We say that an n -vertex random graph G is an instantiation of a 2-level hierarchical stochastic blockmodel with parameters*

$$(n, K_1, \Lambda_1, \pi_1, \{K_2^{(j)}, \Lambda_2^{(j)}, \pi_2^{(j)}\}_{j=1}^{K_1})$$

if

- i. The block membership vector $\pi_1 \in \mathbb{R}^{K_1}$ satisfies $\pi_1(i) \geq 0$ for all $i \in [K_1]$, and $\sum_i \pi_1(i) = 1$;
- ii. The vertex set $V = V(G)$ is the disjoint union of K_1 blocks $V = \mathcal{B}_1^1 \sqcup \mathcal{B}_2^1 \sqcup \dots \sqcup \mathcal{B}_{K_1}^1$, where each vertex $v \in V$ is independently assigned to a block according to a Multinomial($1, \pi_1$) distribution. For each vertex $v \in V(G)$, let $b_v^{(1)}$ be the block that v is assigned to.
- iii. The block probability matrix $\Lambda_1 \in [0, 1]^{K_1 \times K_1}$ is a hollow symmetric matrix. Conditional on the block assignment vector $\vec{b}^{(1)} = (b_v^{(1)})$, for each pair of vertices $\{u, v\} \in \binom{V}{2}$ with $b_u^{(1)} \neq b_v^{(1)}$,

$$\{\mathbf{1}_{u \sim_G v}\} \stackrel{ind.}{\sim} \text{Bernoulli}(\Lambda_1[b_u^{(1)}, b_v^{(1)}]).$$

- iv. For each $j \in [K_1]$, conditional on the block assignment vector $\vec{b}^{(1)} = (b_v^{(1)})$ and $|\mathcal{B}_j^1| > 0$, we have that

$$G[\mathcal{B}_j^1] \sim \text{SBM}(|\mathcal{B}_j^1|, K_2^{(j)}, \Lambda_2^{(j)}, \pi_2^{(j)}).$$

Moreover, conditional on the block assignment vector $\vec{b}^{(1)} = (b_v^{(1)})$ the collection $\{G[\mathcal{B}_j^1]\}_{j=1}^{K_1}$ are mutually independent.

Formally defining the HSBM beyond the second level of the hierarchy is notationally complex, but the main idea is that a k -level HSBM has the same set-up as the 2-level HSBM except that at part *iv.* of the definition, we have

- iv'*. For each $j \in [K_1]$, conditional on the block assignment vector $\vec{b}^{(1)} = (b_v^{(1)})$ and $|\mathcal{B}_j^1| > 0$, we have that

$$G[\mathcal{B}_j^1] \sim \text{k-1 level HSBM}.$$

Moreover, conditional on the block assignment vector $\vec{b}^{(1)} = (b_v^{(1)})$, we have that the collection $\{G[\mathcal{B}_j^1]\}_{j=1}^{K_1}$ are mutually independent.

Recursively applying *iv'*. together with the definition of a 2-level HSBM allows us to define HSBMs of arbitrary depth ($\leq n$ of course).

Remark 2.1. For a k -level HSBM, we shall adopt the notation from the definition of hierarchical graphs already established. Namely, we will denote the j -th block at level i via \mathcal{B}_j^i , where the blocks are labeled in order beginning with those of $B_{(1)}^{i-1}$ and ending with those of $B_{(n_{i-1})}^{i-1}$. We will denote the block-membership function at level i via $\vec{b}^{(i)}$.

While the model complexity of the HSBM can grow quite rapidly as we allow for more structure in each block of the higher level SBMs, the top-down structure does offer complexity savings versus an SBM with the same number of blocks at the bottom-level of the hierarchy. For example, the 1-level HSBM (i.e., the SBM) with K blocks requires

$$\underbrace{\binom{K}{2}}_{\text{for } B} + K + \underbrace{K - 1}_{\text{for } \pi} = O(K^2)$$

parameters to define, while the 2-level HSBM requires

$$\underbrace{\binom{K_1}{2}}_{\text{for } B_1} + \underbrace{K_1 - 1}_{\text{for } \pi_1} + \sum_{j=1}^{K_1} \left[\underbrace{\binom{K_2^{(j)}}{2}}_{\text{for } B_2^{(j)}} + K_2^{(j)} + \underbrace{K_2^{(j)} - 1}_{\text{for } \pi_2^{(j)}} \right] = O(K_1^2 + \sum_j (K_2^{(j)})^2)$$

parameters. As a simple example, if $K_1 = 3$ and each $K_2^{(j)} = 3$, then the HSBM has 9 blocks at its bottom level and requires 29 parameters while a 9 block SBM requires 53 parameters. The complexity of an HSBM can be further reduced by enforcing repeated motif structure [26], though we do not explore this further herein.

Remark 2.2. Consider a k -level HSBM G . Letting $(n_i)_{i=1}^k$ denote the number of blocks at level i in the hierarchy of G , so that (for example)

$$\begin{aligned} n_1 &= K_1 \\ n_2 &= \sum_{i=1}^{K_1} K_2^i \\ n_3 &= \sum_{i=1}^{K_1} \sum_{j=1}^{K_2^i} K_3^{(j,i)} \\ n_4 &= \sum_{i=1}^{K_1} \sum_{j=1}^{K_2^i} \sum_{\ell=1}^{K_3^{(j,i)}} K_4^{(\ell,j,i)} \\ &\vdots \end{aligned}$$

(where $K_3^{(j,i)}$ is the number of blocks in the j -th block of the i -th block of G ; $K_4^{(\ell,j,i)}$ is the number of blocks in the ℓ -th block of the j -th block of the i -th block of G ; etc...) and conditioning on all blocks being non-empty at each level of the hierarchy, G defines a distribution over the subset of k -level hierarchical graphs

$$\mathcal{HG}_n^{\vec{n}} := \{(g, H) \in \mathcal{HG}_n \mid \text{the signature of } H \text{ is } \vec{n}\}.$$

We then have that (for example), $H(v, i) = \vec{b}_v^{(i)}$ for all $v \in [n]$ and $i \in [k]$.

2.2.2 Hierarchical Subgraph Nomination

A key component to the hierarchical subgraph nomination (HSN) inference task is the notion of subgraphs of interest within and across the network pair. This is easily accomplished in non-random settings, where a fixed set of indices can be used to define the subgraphs of interest within and across networks. In order to expedite this in random networks, for a fixed pair of signatures \vec{n} and \vec{m} , we will consider distributions restricted to $\mathcal{HG}_n^{\vec{n}} \times \mathcal{HG}_m^{\vec{m}}$; this will allow us to define a consistent set of indices for subgraphs of interest across the random network pair.

In hierarchical subgraph nomination, we consider a pair of hierarchical graphs $(g_1, H_1) \in \mathcal{HG}_n^{\vec{n}}$ and $(g_2, H_2) \in \mathcal{HG}_m^{\vec{m}}$ where H_1 and H_2 are unobserved and only the graphs g_1 and g_2 are observed. We are additionally given a set of “training” subgraphs of interest in g_1 , denoted

$$T_1 = \{B_{s_2,1}^{s_1}\}_{s=(s_1,s_2) \in S_1}$$

where S_1 is a set of ordered pair indices $S_1 = \{s = (s_1, s_2)\}$ of the given subgraphs of interest, with s_1 denoting the level and s_2 the index of the subgraph in H_1 . Note that the second index in the subscript of $B_{\bullet,1}^{\bullet}$ is used to denote the subgraph in g_1 , whereas $B_{\bullet,2}^{\bullet}$ will be used to indicate subgraphs in the hierarchy of g_2 . Note that the possible indices of the seed graphs depends on the structure of H_1 , and so we will explicitly tether these two in the sequel, writing $((g_1, H_1), S_1)$, and writing $\mathcal{HGS}_n^{\vec{n}}$ for the collection of all such feasible triples.

The aim then is to

1. First estimate the latent hierarchical structure H_2 of g_2 ; we will denote this estimate via \widehat{H}_2 , and we will let

$$\widehat{B}_{j,2}^i = \{v \in V(g_2) | \widehat{H}_2(v, i) = j\}.$$

Let the collection of all subgraphs in the partition defined by \widehat{H}_2 be denoted \widehat{B} .

2. Compute dissimilarity measurements

$$\Delta : T_1 \times \widehat{B} \mapsto [0, 1]$$

between each subgraph of interest in (g_1, H_1) and each subgraph defined by \widehat{H}_2 . Note that Δ ideally is a function that can compute the dissimilarity between any graph of order up to n and any graph of order up to m ; and the larger the value of Δ between two graphs, the more dissimilar the networks. As Δ needs to compute dissimilarities across graphs of different sizes and orders, it may encompass a collection of dissimilarity measures.

After a few preliminary definitions, we will be ready to define a HSN scheme.

Definition 2.4. For a k -level hierarchical graph (g, H) and $i \in [k]$, let $\mathcal{T}_{g,i}^H$ denote the set of all total orderings of B^i . Let $\mathcal{T}_g^H = \bigotimes_{i=1}^k \mathcal{T}_{g,i}^H$.

For example, in the hierarchical subgraph depicted in Figure 2, we have

$$\mathcal{T}_{g,2}^H = \left\{ \begin{bmatrix} B_1^2 \\ B_2^2 \\ B_3^2 \end{bmatrix}, \begin{bmatrix} B_1^2 \\ B_3^2 \\ B_2^2 \end{bmatrix}, \begin{bmatrix} B_2^2 \\ B_1^2 \\ B_3^2 \end{bmatrix}, \begin{bmatrix} B_2^2 \\ B_3^2 \\ B_1^2 \end{bmatrix}, \begin{bmatrix} B_3^2 \\ B_1^2 \\ B_2^2 \end{bmatrix}, \begin{bmatrix} B_3^2 \\ B_2^2 \\ B_1^2 \end{bmatrix} \right\}$$

where

$$\begin{bmatrix} B_i^2 \\ B_j^2 \\ B_k^2 \end{bmatrix}$$

is shorthand for the ordering

$$B_i^2 > B_j^2 > B_k^2.$$

An example element of \mathcal{T}_g^H is given by

$$([B_1^1], [B_3^2, B_2^2, B_1^2], [B_2^3, B_9^3, B_8^3, B_1^3, B_3^3, B_6^3, B_5^3, B_7^3, B_4^3]).$$

As in the case of vertex nomination, if vertex labels in (g_2, H_2) are uninformative, then an HSN must account for the indistinguishability of subgraphs with isomorphic structure. To wit, we have the following definition: For a k -level hierarchical network (g, H) and $i \in [k]$, $j \in [n_i]$, we define

$$\mathfrak{J}(B_j^i; g) = \{\ell \in [n_i] \mid B_\ell^i \subset B_{(j)}^{i-1} \text{ and there exists an automorphism } \sigma \text{ of } g \text{ with } \sigma(B_\ell^i) = B_j^i\}.$$

These are indices of the elements of the partition at level i that are indistinguishable from B_j^i without further information/supervision, and it is sensible to require that a HSN rank all these subgraphs as equally interesting. In vertex nomination, accounting for label uncertainty was achieved by means of an obfuscation function; in HSN, the uncertainty is not at the level of labels so much as at the level of subgraphs and this this can be achieved by further requiring the dissimilarity Δ satisfy

$$\Delta(B_{s_2,1}^{s_1}, \cdot) \text{ is constant over graphs indexed by } \mathfrak{J}(\widehat{B}_{j,2}^i; g_2) \text{ for each } s = (s_1, s_2) \in S_1. \quad (1)$$

We are now ready to define hierarchical subgraph nomination schemes formally.

Definition 2.5. [*Hierarchical Subgraph Nomination Scheme (HSN)*] Let $((g_1, H_1), S_1) \in \mathcal{HGS}_n^{\widehat{n}}$ and $((g_2, H_2), S_2) \in \mathcal{HGS}_m^{\widehat{m}}$ and let T_1 be the parts of H_1 indexed by S_1 . A Hierarchical subgraph nomination scheme is composed of two parts:

- i. An estimator $\widehat{H}_2 = \widehat{H}_2(g_1, g_2, T_1)$ of the hierarchical clustering of g_2 provided by H_2 ; let the signature of \widehat{H}_2 be denoted $\widehat{m}_2 = (\widehat{m}_{k,2})$;
- ii. A dissimilarity Δ satisfying Eq. (1) which produces a ranking scheme $\Phi_{n,m}$, where

$$\Phi_{n,m} \left(g_1, g_2, T_1, \widehat{H}_2 \right) \in \mathcal{T}_{g_2}^{\widehat{H}_2}.$$

For each level i of \widehat{H}_2 , the subgraphs are ordered in $\Phi_{n,m}$ via increasing value of

$$\min_{s=(s_1,s_2) \in S_1} \Delta(B_{s_2,1}^{s_1}, \widehat{B}_{j,2}^i),$$

with ties broken in a fixed but arbitrarily manner.

2.3 Loss in HSN Schemes

The goal of HSN is to effectively query g_2 given limited training resources from g_1 . Given the resources required for a user to verify the interestingness of the returned subgraphs, we seek to maximize the probability that a priori unknown subgraphs of interest in g_2 are close to the top of the returned rank list.

For evaluation purposes, it is necessary (at least in theory) to be able to compare the true-but-unknown subgraphs of interest in $((g_2, H_2), S_2) \in \mathcal{HGS}_m$ with elements of the HSN ranked list. In order to account for the fact that the dissimilarity used to construct the HSN scheme may be mis-specified (i.e., not captured exactly), the dissimilarity for verification will be denoted Δ_E (the dissimilarity used for evaluation that defines the true but unknown subgraphs of interest), though we do not discount the possibility that $\Delta_E = \Delta$ for any given scheme.

A logical loss function for HSN is motivated by the concept of precision in information retrieval. As the goal of HSN is to efficiently query large networks for structures of interest, at a given level k , considering precision at i for $1 < i \ll \hat{m}_{k,2}$ enables us to model the practical loss associated with using a HSN scheme to search for $\{B_{s_2,2}^{s_1}\}_{(s_1,s_2) \in S_2}$ in (g_2, H_2) given limited resources. There are two levels to the loss function for a given scheme $\Phi_{n,m} = (\hat{H}_2, \Delta)$:

- i. The error in approximating H_2 via \hat{H}_2 ;
- ii. Given \hat{H}_2 , the potential mismatch between Δ and Δ_E .

Our loss function will account for these error sources as follows. Let F be a distribution supported on $\mathcal{HGS}_n \times \mathcal{HGS}_m$, and let

$$((G_1, H_1), (G_2, H_2)) \sim F.$$

Consider fixed subgraph of interest index sets S_1 for G_1 and S_2 for G_2 , and let T_1 (resp., T_2) be those subgraphs in (G_1, H_1) (resp., (G_2, H_2)) indexed by S_1 (resp., S_2). Let $\Phi_{n,m} = (\hat{H}_2, \Delta)$ be an HSN scheme and let the ranking provided at level k of $\Phi_{n,m}$ be denoted via $\Phi_{n,m}^k$ (with the implicit assumption that this is an empty list if $\hat{m}_{k,2} = 0$).

Definition 2.6 (HSN loss function, level- (i, k) error at hierarchical level). *With setup as above, for $i, k < n$ we define the level- (i, k) nomination loss with threshold $t > 0$ under dissimilarity Δ_E via (where to ease notation, we will use $\Phi_{n,m}^k$ for $\Phi_{n,m}^k(g_1, g_2, T_1, \hat{H}_2)$ and $\Phi_{n,m}^k[j]$ the j -th ranked subgraph in this list)*

$$\ell_{i,k,t} := \ell_{i,k,t}(\Phi_{n,m}, g_1, H_1, S_1, g_2, H_2, S_2, \Delta_E)$$

where

$$\ell_{i,k,t} := \begin{cases} \frac{1}{\min(i, \hat{m}_{k,2})} \sum_{j=1}^{\min(i, \hat{m}_{k,2})} \mathbf{1} \left\{ \bigcap_{(s_1, s_2) \in S_2} \{\Delta_E(\Phi_{n,m}[j], B_{s_2,2}^{s_1}) > t\} \right\} & \text{if } \hat{m}_{k,2} > 0 \\ 1 & \text{if } \hat{m}_{k,2} = 0 \end{cases} \quad (2)$$

For distribution F as above, the level- (i, k) error with threshold $t > 0$ under dissimilarity Δ_E of $\Phi_{n,m}$ for recovering S_2 is defined to be $L_{i,k,t} = \mathbb{E}_F(\ell_{i,k,t})$. Letting $\mathfrak{S}_{n,m}$ be the collection of

all HSN schemes (i.e., the set of all ordered pairs of estimators and dissimilarities (\widehat{H}_2, Δ)), the Bayes optimal level- (i, k) scheme with threshold $t > 0$ under dissimilarity Δ_E is defined to be any scheme that achieves the Bayes' error, which here is defined to be

$$\min_{\Phi_{n,m} \in \mathfrak{S}_{n,m}} \mathbb{E}_F(\ell_{i,k,t}(\Phi_{n,m}))$$

While the number of possible dissimilarities is indeed uncountably infinite, there are nonetheless a finite number of possible rankings that can be achieved via a combination of \widehat{H}_2 and Δ (hence min rather than inf in the Bayes error definition), and so the Bayes error is indeed achieved by at least one such pair.

2.4 User-in-the-loop Supervision

Interactive machine learning, via incorporating user-in-the-loop supervision, can lead to an enhanced user experience and better downstream inference performance [3]. In subgraph nomination, the need for user-in-the-loop supervision can be understood as follows. Consider nominating in $((g_2, H_2), S_2)$ at level k , where $S_2 = \{(k, \ell)\}$, and $|\mathfrak{J}(B_{\ell,2}^k; g_2)| > 1$. Even if \widehat{H}_2 agrees with H_2 at level k , there are multiple subgraphs in (g_2, H_2) that are isomorphic to the unknown subgraph of interest, and the HSN scheme has no information available to distinguish these. In this setting, it is reasonable to model the relative order of the elements in $\mathfrak{J}(B_{\ell,2}^k; g_2)$ in an HSN scheme as (effectively) uniformly random. For example, if $|\mathfrak{J}(B_{\ell,2}^k; g_2)| = c$, then considering top h of our nomination list ($h < c$), a scheme that identifies the correct structure for $B_{\ell,2}^k$ would still have probability

$$\frac{\binom{c-1}{h}}{\binom{c}{h}} = \frac{c-h}{c} = 1 - \frac{h}{c}$$

of not finding $B_{\ell,2}^k$. This can be mitigated by the following user-in-the-loop system:

- i. The user can take a limited number of single vertex inputs and can output whether that vertex is interesting or not (i.e., part of an interesting subgraph). This output can be modeled as error-free (oracle-user) or errorful.
- ii. The supervision can then be used to re-rank the subgraphs in the nomination scheme.

While practically, we do not suspect that there will be many perfect matches to the subgraphs of interest in the hierarchy provided by H_2 , it may be the case that there are many subgraphs “close” to the subgraph of interest in the (possibly lossy) estimate \widehat{H}_2 , in which case this supervision is equally necessary.

What follows is a formalization of the above heuristic. We first define the concept of a user-in-the-loop; noting that our definition is not the most general, as we focus in our analysis on binary users; i.e., they can only output 1 (yes) or 0 (no) for the interestingness of a vertex. In general, one might allow for the user to use a rating system with more levels, or even add a continuous space for responses.

Definition 2.7 (VN User). *Let $(g_1, H_1) \in \mathcal{HGS}_n$ with indices of interest S_1 and $(g_2, H_2) \in \mathcal{HGS}_m$ with indices of interest S_2 . Let $(\theta, \gamma) \in [0, 1] \times [0, 1]$ and $t \in \mathbb{Z} > 0$ with $t < m$. We define the capacity t , HSGN user-in-the-loop for $((g_2, H_2), S_2)$ with parameters (θ, γ) (denoted U_t) as follows:*

i. Letting Ω be the underlying sample space, the user is a function

$$U_t : \mathcal{T}_{V_2, t} \times \Omega \mapsto \{0, 1\}^t$$

where $\mathcal{T}_{V_2, t}$ is the set of ordered t -tuples of distinct elements from $V_2 = V(g_2)$. Note that dependence on Ω will be suppressed when appropriate.

ii. For each $\eta \in \mathcal{T}_{V_2, t}$ and $x \in \{0, 1\}^t$, we define

$$\begin{aligned} \mathbb{P}(U_t(\eta) = x) = \prod_{i=1}^t \left[\left(\mathbb{1}\{\eta_i \in \bigcup_{(s_1, s_2) \in S_2} B_{s_2, 2}^{s_1}\} \theta^{x_i} (1 - \theta)^{1-x_i} \right) \right. \\ \left. + \left(\mathbb{1}\{\eta_i \notin \bigcup_{(s_1, s_2) \in S_2} B_{s_2, 2}^{s_1}\} \gamma^{x_i} (1 - \gamma)^{1-x_i} \right) \right] \end{aligned} \quad (3)$$

In essence, the user has independent binary components where the Bernoulli success probabilities depend only on the membership (or lack thereof) in a subgraph of interest.

For a given $((g_2, H_2), S_2)$ and t , we define the set of all such users by $\mathfrak{U}_t = \mathfrak{U}_{((g_2, H_2), S_2), t}$.

Effectively, the HSN user-in-the-loop outputs a sequence of $\{0, 1\}$ values, one for each vertex in a training set η . An output of 1 is considered the positive answer, i.e. an interesting vertex; for vertices in $\bigcup_{(s_1, s_2) \in S_2} B_{s_2, 2}^{s_1}$, this is a correct answer, and an error otherwise. An output of 0 is the negative answer meaning that this vertex is not of interest; for vertices not in $\bigcup_{(s_1, s_2) \in S_2} B_{s_2, 2}^{s_1}$, this is a correct answer and is an error otherwise. This allows us to simultaneously model oracle users ($\theta = 1$, and $\gamma = 0$) and errorful users ($\theta < 1$, and $\gamma > 0$). The capacity of the user (i.e., t) allows us to model the practical setting in which user-in-the-loop resources are costly and only limited supervision is available.

Users can be incorporated into HSN schemes as follows.

Definition 2.8. *User Aided HSN Scheme (UHSN)* Consider the setting in Definition (2.5). Let $t \leq n_j^{(2)}$ and $U_t \in \mathfrak{U}_t$. Consider an HSN $\Phi_{n, m} = (\widehat{H}_2, \Delta)$, and let η be an ordered t -tuple of distinct elements of $V_2 = V(g_2)$. For each k , U_t acts on $\Phi_{n, m}^k$ as follows:

i. Given η , U_t is distributed according to Eq. 3. Let the output of the user process be denoted $x \in \{0, 1\}^t$.

ii. Let

$$\begin{aligned} I_k &:= \{\ell \in [\widehat{m}_k] \text{ s.t. more than half of the vertices in } \eta \cap \widehat{B}_{\ell, 2}^k \\ &\quad \text{were labeled interesting (i.e., as 1) by the user}\} \\ N_k &:= \{\ell \in [\widehat{m}_k] \text{ s.t. at least half of the vertices in } \eta \cap \widehat{B}_{\ell, 2}^k \\ &\quad \text{were labeled as not interesting (i.e., as 0) by the user}\} \end{aligned}$$

If $\eta \cap \widehat{B}_{\ell, 2}^k = \emptyset$, then $\ell \notin I_t \cup N_t$.

iii. Let the indices of I_t be indexed via $(i_1, \dots, i_{|I_t|})$ where (according to $\Phi_{n,m}^k$)

$$\widehat{B}_{i_1,2}^k > \widehat{B}_{i_2,2}^k > \dots > \widehat{B}_{i_{|I_t|},2}^k.$$

Similarly index N_t via $(n_1, \dots, n_{|N_t|})$, and $M_t := [\widehat{m}_k] \setminus \{I_t, N_t\}$ (the unsupervised subgraph indices) via $(m_1, \dots, m_{|M_t|})$. The user improved ranking is then given by

$$\begin{aligned} \Phi_{n,m}^{k,U} = & \left(\widehat{B}_{i_1,2}^k > \widehat{B}_{i_2,2}^k > \dots > \widehat{B}_{i_{|I_t|},2}^k > \widehat{B}_{m_1,2}^k > \widehat{B}_{m_2,2}^k > \dots \right. \\ & \left. > \widehat{B}_{m_{|M_t|},2}^k > \widehat{B}_{n_1,2}^k > \widehat{B}_{n_2,2}^k > \dots > \widehat{B}_{n_{|N_t|},2}^k \right). \end{aligned}$$

Remark 2.3. We note here the possibility of even an oracle user introducing large errors into a ranking scheme based on an approximate \widehat{H}_2 . Indeed, even if $\widehat{B}_{\ell,2}^k$ is very similar to an interesting subgraph in g_1 according to Δ , it is still possible that uninteresting vertices are chosen to provide to the user and $\ell \in N_t$. This can be mitigated by choosing multiple vertices from each of some of the top ranked subgraphs for the user to evaluate.

Remark 2.4. For iterative applications of the user-in-the-loop, we can sequentially run the user-in-the-loop, first on the output of $\Phi_{n,m}$, then on $\Phi_{n,m}^U$ (with t new user training points), and so on.

2.4.1 The (Theoretical) Benefit of the User-in-the-loop

We turn our attention now to take a look at the theoretical benefit of the user-in-the-loop in the setting of HSN. As in the motivating example for the user, the setting for this section will be as follows. Letting $(g_1, H_1) \in \mathcal{HGS}_n$ and $(g_2, H_2) \in \mathcal{HGS}_m$ with respective interesting index sets S_1 and S_2 , consider a HSN scheme $\Phi_{n,m}$ with $\widehat{H}_2 = H_2$. Consider the nomination provided by $\Phi_{n,m}^k$ and the simple setting in which $S_2 = \{(k, \ell)\}$ with $|\mathfrak{J}(B_{\ell,2}^k; g_2)| = c > 1$. In this setting, it is reasonable to model the relative order of the elements in $\mathfrak{J}(B_{\ell,2}^k; g_2)$ in an $\Phi_{n,m}^k$ as (effectively) uniformly random (though in practice, they are a fixed arbitrary order).

Theorem 2.1. *Given the setup above where the scheme $\Phi_{n,m}$ effectively ranks the elements of $\mathfrak{J}(B_{\ell,2}^k; g_2)$ uniformly at random at the top of the rank list, let $t \leq c < m_k$ be the capacity of the user-in-the-loop. Consider any training set for the user where η contains exactly one element of each $\Phi_{n,m}^k[h]$ with $1 \leq h \leq t$. Let E_h denote the event that $\Phi_{n,m}^U$ ranks $B_{\ell,2}^k$ not in the top h . Considering $c > t, h$, we have the following.*

i. Let U_t be an oracle user, then $\mathbb{P}(E_h) = \max(1 - \frac{h+t}{c}, 0)$.

ii. Let $(\theta, \gamma) = (1 - p, 0)$ for $p < 1$, then

– If $t + h \leq c$, then $\mathbb{P}(E_h) = 1 - \frac{h}{c} - (1 - p)\frac{t}{c}$; note that this is strictly less than $1 - h/c$ for all $p \in (0, 1)$.

– If $t + h > c$, then $\mathbb{P}(E_h) = \frac{tp}{c}$; note that if $p < (c - h)/t$, this is strictly less than $1 - h/c$.

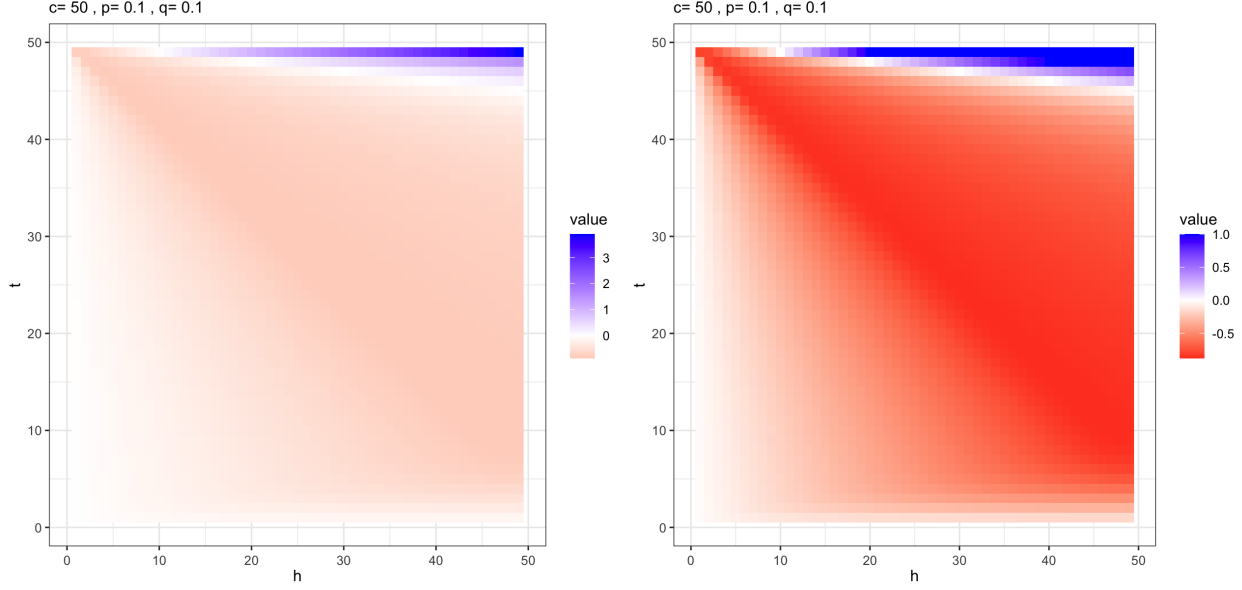


Figure 3: For $c = 50$ we plot (for $h, t \in \{1, 2, \dots, 49\}$) the relative loss $R(c, t, h, p, q)$ in the setting of Theorem 2.1 part (iii) in the left panel $\min(R(c, t, h, p, q), 1)$ in the right panel.

iii. Let $(\theta, \gamma) = (1 - p, q)$ for $p < 1$ and $q > 0$. Then, letting $F(i; n, p)$ be the CDF of a Binomial(n, p) random variable evaluated at i , we have

- If $h + t \leq c$, and $t \leq h$, then $\mathbb{P}(E_h) = 1 - \frac{h}{c} - \frac{(1-p-q)t}{c}$; note that if $p + q < 1$, this is less than $1 - \frac{h}{c}$.
- If $h + t > c$, and $t \leq h$, then $\mathbb{P}(E_h) = \frac{pt}{c} + \frac{1}{c} \sum_{i=1}^{c-h} F(i-1; t, 1-q)$; this is upper bounded by $(p+q)t/c$ and if $(p+q) < (c-h)/t$, this is strictly less than $1 - h/c$.
- If $h + t \leq c$, and $t > h$, then

$$\begin{aligned} \mathbb{P}(E_h) &= 1 - \frac{h}{c} - \frac{(1-p)t}{c} + \frac{1-p}{c} \sum_{i=1}^{t-h} F(i-1; h+i-1, 1-q) \\ &\quad + \frac{1}{c} \sum_{i=t-h+1}^t F(i-1; t, 1-q) \end{aligned}$$

Note that a rough upper bound of this is given by $1 - h/c + qt/c - (1-p)h/c$, and if $qt < (1-p)h$, this is strictly less than $1 - h/c$.

- If $h + t > c$, and $t > h$, then

$$\mathbb{P}(E_h) = \frac{pt}{c} + \frac{1-p}{c} \sum_{i=1}^{t-h} F(i-1; h+i-1, 1-q) + \frac{1}{c} \sum_{i=t-h+1}^{c-h} F(i-1; t, 1-q)$$

Note that a rough upper bound of this is given by $\frac{(1+q)t - (1-p)h}{c}$, and if $(1+q)t + ph < c$, this is strictly less than $1 - h/c$.

We, perhaps surprisingly, see that there are p and q values that guarantee improvement (over the user-in-the-loop-free setting) in all cases. The conditions in part *iii*. bear further consideration. The interaction of p, q, h, t here is nuanced, and is most easily analyzed numerically, as is shown in Figures 3 and 4. Letting $L(c, t, h, p, q)$ denote the loss from Theorem 2.1 part (iii) (where we can interpret this in the context of Definition 2.6 by considering Δ as a 0/1 oracle dissimilarity function), for $c = 50$ we plot the relative loss improvement,

$$R(c, t, h, p, q) = \frac{L(c, t, h, p, q) - (1 - h/c)}{1 - h/c}, \quad (4)$$

for h between 1 and 49 (on the y -axis), and t between 1 and 49 (on the x -axis). Different panels correspond to different values of p (varies by row) and q (varies by column). Note that in Figures 3, we plot the relative loss in the left panel $R(c, t, h, p, q)$ and $\min(R(c, t, h, p, q), 1)$ in the right panel; this truncating aids in distinguishing the areas of improvement from those where $R(c, t, h, p, q) > 0$.

In each plot, darker red areas correspond to parameter settings where the loss is improved with user-supervision, and darker blue areas to parameter settings where the loss is increased with user-supervision (due to the user error). A few trends are clear from the figures. Unsurprisingly, supervision becomes detrimental (i.e., more supervision leads to more loss) as p and q increase and $q \geq 0.5$, although the loss appears to be more tolerant of higher values of p than it is of q . In all cases, large values of t and h simultaneously lead to training becoming less effective, though $h < t$ seems to yield resilience to larger user-supervised loss for all p, q pairs.

In the event that the hierarchical clustering is noisily recovered in g_2 (i.e., $\widehat{H}_2 \neq H_2$), even the supervision provided by an oracle user-in-the-loop may be worse than no extra supervision. Indeed, consider the setting where $S_2 = \{(k, \ell)\}$ and

$$\alpha = \frac{|\widehat{B}_{\ell,2}^k \cap B_{\ell,2}^k|}{|\widehat{B}_{\ell,2}^k|}; \quad \beta = \min_{i \neq \ell} \frac{|\widehat{B}_{i,2}^k \cap B_{\ell,2}^k|}{|\widehat{B}_{i,2}^k|},$$

then, adopting the notation and setting above, the probability that $\widehat{B}_{\ell,2}^k$ is not ranked in the top h after oracle U_t supervision is bounded below by the probabilities in part (iii) of Theorem 2.1 with $p = \alpha$ and $q = \beta$. In particular, there are values of α and β under which this error is worse than $1 - h/c$ (the error sans additional supervision).

3 Simulations and Real Data Experiments

We now provide empirical evidence for the theory we have outlined. Namely, we will show through simulations and real data examples the impact of a user-in-the-loop. We first consider simulations where graphs are drawn from an HSBM distribution. In this setting we evaluate our methodology on the task of nominating subgraphs with a similar motif to our subgraph of interest. We then consider 57 pairs of analyzed human neural connectomes for which brain regions (i.e., communities) are well defined and the community for each voxel is known. We evaluate our methodology on the task of nominating the same brain region within a given pair of connectomes with varying levels of a user-in-the-loop.

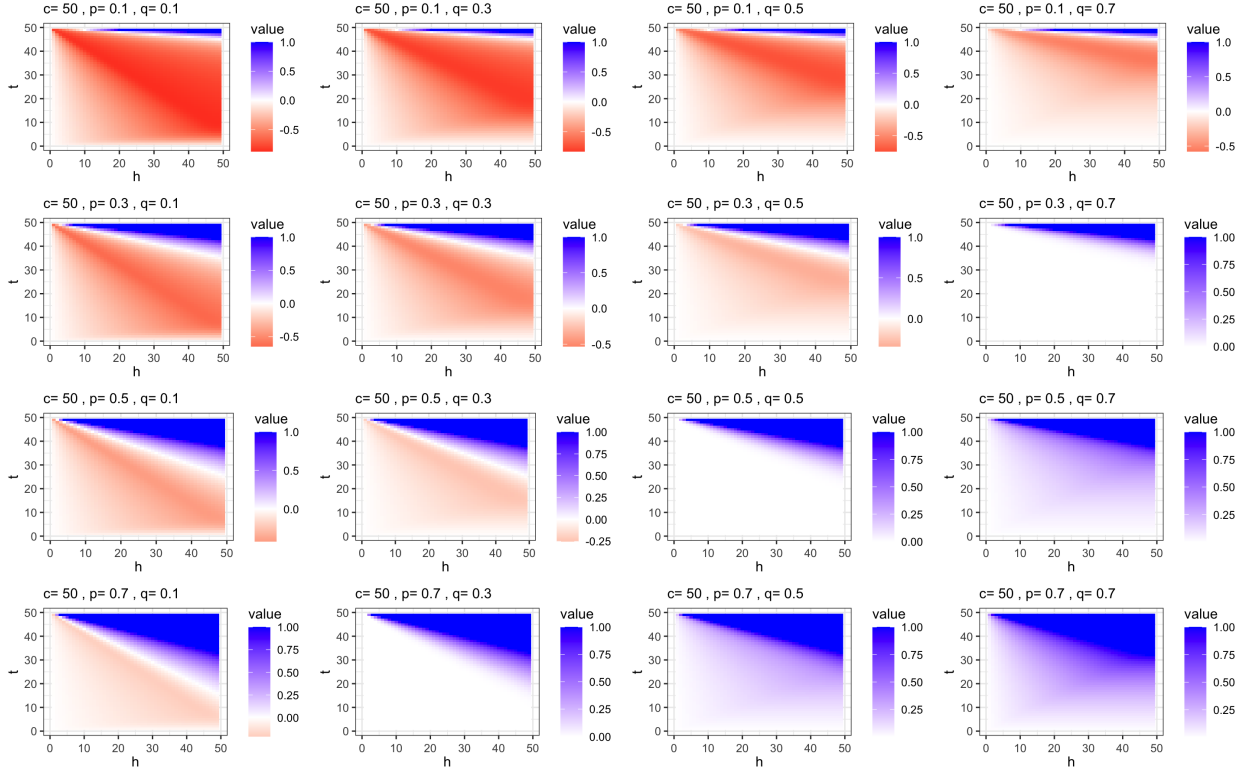


Figure 4: For $c = 50$ we plot (for $h, t \in \{1, 2, \dots, 49\}$) $\min(R(c, t, h, p, q), 1)$ for the loss function in the setting of Theorem 2.1 part (iii) and R defined in Equation (4). Different panels correspond to different values of p and q .

3.1 Simulations

In this section we will first provide a complete description of the model and procedures that were employed to test our theory in a simulated data setting. We then discuss results and how they fit within our theory.

3.1.1 Model description

For our first example, we consider nominating within the Hierarchical Stochastic Blockmodel setting of [26]. We consider sampling from a 2-level HSBM that has 16 blocks in the first level and 3 sub-blocks in each of the first level blocks (so that this model can also be realized as a 48 block standard SBM). Further, the blocks of the first level belong to one of three motifs B_1 , B_2 , or B_3 , with constant cross-community connection probability $p = 0.01$ for the first level. Formally, we are sampling from the following 2-level HSBM:

- i. There are $K_1 = 16$ blocks in the first level of the hierarchy, and the size of the blocks is i.i.d. $10 * [20 + 50 * Unif(0, 1)]$; note that this differs slightly from the random block assignment HSBM defined previously.

- ii. The motifs $\mathbf{B}_i \in \mathbb{R}^{3 \times 3}$ for $i = 1, 2, 3$ are i.i.d. samples satisfying

$$\mathbf{B}_i = X_i^T X_i \text{ where } X_i \in \mathbb{R}^{3 \times 3} \text{ satisfies } X_i[\cdot, j] \stackrel{i.i.d.}{\sim} Dirichlet(1, 1, 1);$$

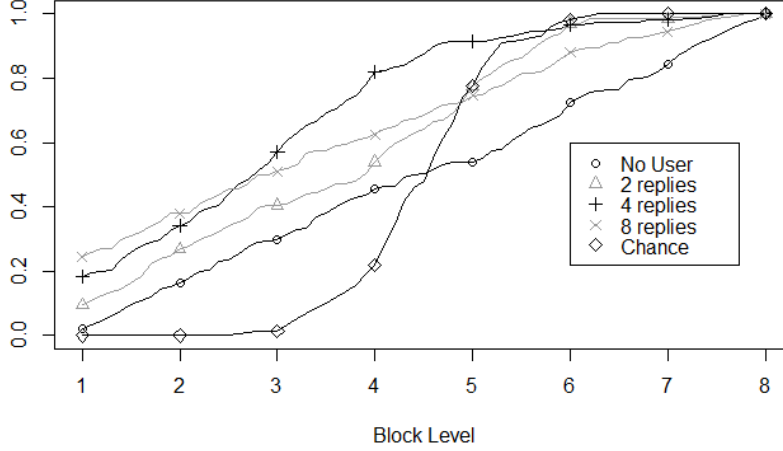


Figure 5: We consider 2000 Monte Carlo replicates of distributions as in Section 3.1.1, and from each distribution, we generate 100 networks. We use Method 1, and performance with an oracle user (varying the replies for the user; i.e., the amount of supervision provided) and the chance algorithm are compared. In all cases, we plot the proportion of trials (y-axis) that ranked the correct block in the n th place (x-axis) which represents $1 - L_n(\phi, B^*)$.

- iii. For each $j \in [16] \setminus \{9\}$, we have $B_2^j = \mathbf{B}_i$ independently with probability $1/3$ for $i = 1, 2, 3$. B_2^9 is set to equal B_2^1 ;
- iv. In the second level of the hierarchy ($K_2^j = 3$ for all j), the block sizes are defined via (where $\lfloor \cdot \rfloor_1$ rounds the number to the nearest tenth)

$$|b_{(j,i)}^{(2)}| = |\{v \in V | b^{(1)}(v) = j, b^{(2)}(v) = i\}| \stackrel{i.i.d.}{\sim} |b_j^{(1)}| \cdot \lfloor \text{Dirichlet}(\omega) \rfloor_1(i), i < 3$$

where the entries of $\omega = (\omega_1, \omega_2, \omega_2)$ are

$$\omega_i \stackrel{i.i.d.}{\sim} \text{Unif}(2, 10).$$

Lastly, we set

$$|b_{(j,3)}^{(2)}| = |\{v \in V | b^{(1)}(v) = j, b^{(2)}(v) = 3\}| = |b_j^{(1)}| - |b_{(j,i)}^{(2)}| - |b_{(j,i)}^{(2)}|$$

This particular parameterization is chosen to produce different motifs that stress our HSGN framework by producing motifs that are very similar, and motifs where the block structure is extremely subtle (i.e., close to flat), and cases where both these problems happen, as it draws from a distribution in which it is not uncommon that the motifs turn out to be extremely similar and/or very flat.

The block structure was inferred by clustering via Gaussian mixture modeling after embedding, utilizing the **R** package **Mclust** [14] to cluster the graph we are nominating from into 8 sub-graphs. After that, we use two different methods to infer similarity. The first approximates Δ via the value of the non-parametric test statistic of [40] computed between

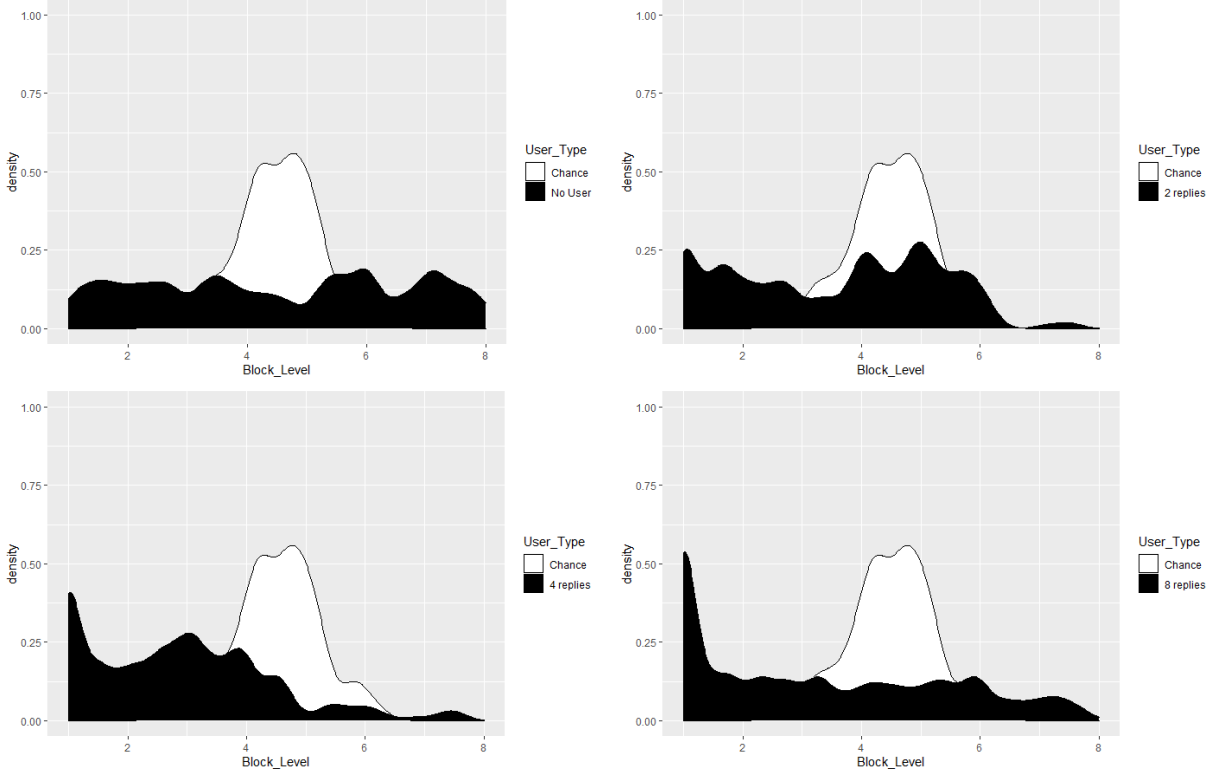


Figure 6: We consider 2000 Monte Carlo replicates of distributions as in Section 3.1.1, and from each distribution, we generate 100 networks. We use Method 1, and performance with an oracle user (varying the replies for the user; i.e., the amount of supervision provided) and the chance algorithm are compared. We plot the density of all trials (y-axis) that ranked the correct block in the n th place (x-axis).

re-embeddings of each inferred community (as in [26]); simulation results are shown in Figures 5 and 6. We will call this *Method 1* in the sequel. The second approximates Δ between communities i and j via the scaled graph matching pseudo-distance [13],

$$1 - \frac{\min_{P \in \Pi(n)} \|A_i - PA_j P^T\|_F^2}{\frac{1}{n!} \sum_{P \in \Pi(n)} \|A_i - PA_j P^T\|_F^2}$$

where either A_i (the induced subgraph of community i) or A_j has been appropriately padded as in [10]); results are shown in Figures 7 and 8. We will call this *Method 2* in the sequel.

The user replies are those of an oracle. However, as discussed previously since we do perfectly recover the true network partition (rather than using an estimate of the true network partition), our user could still end up being errorful. In particular, the user could be asked to rank vertices that are not in the subgraph of interest. This exemplifies the behavior characterized by *iii* of Theorem 2.1, albeit with a different q for each of the blocks. Another significant difference in the scheme of the simulation is that the nomination process takes the first affirmative reply as the correct community and returns the others in their order as is.

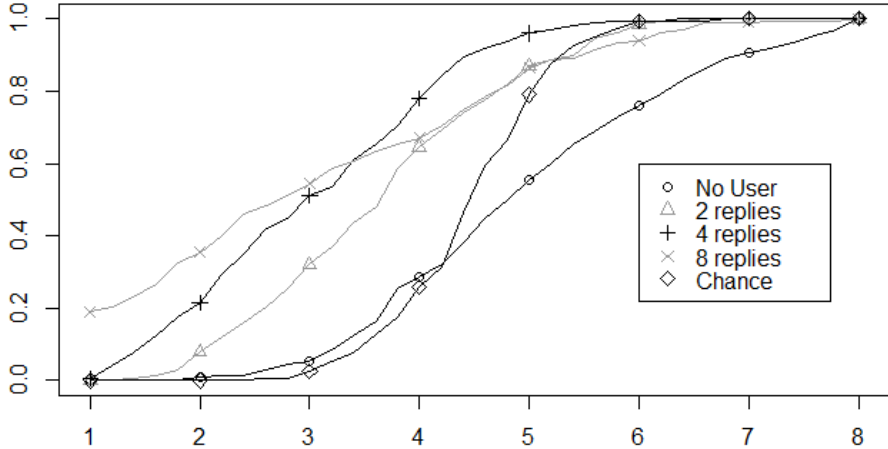


Figure 7: We consider 2000 Monte Carlo replicates of distributions as in Section 3.1.1, and from each distribution, we generate 100 networks. We use Method 2, and performance with an oracle user (varying the replies for the user; i.e., the amount of supervision provided) and the chance algorithm are compared. We plot the proportion of trials (y-axis) that ranked the correct block in the n th place (x-axis) which represents $1 - L_n(\phi, B^*)$

3.1.2 Results & Discussion

In this section we will go over the results of the experiments we described. The aim is to bolster the claims in the theoretical results with experimental results, as such we will have a special focus on the features that are iconic from the theory. First we start with Method 1, the experiment that uses the test statistic form [40] to estimate the dissimilarity function.

In Figure 5 we can see that the user training provides an improvement over the original algorithm (“No user”), as suggested by Theorem 2.1, with more training often yielding superior performance. Moreover, especially for small x -values, the the algorithm outperforms a chance ranking of the obtained blocks. Interestingly, we see that more user-supervision is not always better. Indeed, as mentioned previously, in our regime of lossy block recovery additional supervision can be deleterious. Figure 6 elucidates this finding further from the perspective of the distribution density of the correct block in each position. We notice that as user-supervision increases the distribution are shifted towards putting the correct block in the first position. We also notice the trend predicted by Figure 4, as we increase h (the nomination error level) the ideal value of t (user-provided replies) is decreasing, and less supervision is preferred. We see this, as the curves with less supervision overtake those of higher supervision as we plot $1 - L_n(\phi, B^*)$. However we note that here the value of q is not constant and hence the minimizers of the loss function do not not adhere to the figure exactly. In Figures 7 and 8 we see similar trends using Method 2. Here the main contribution to the error of the methods is the misclustering of the vertices in the initial GMM step, and

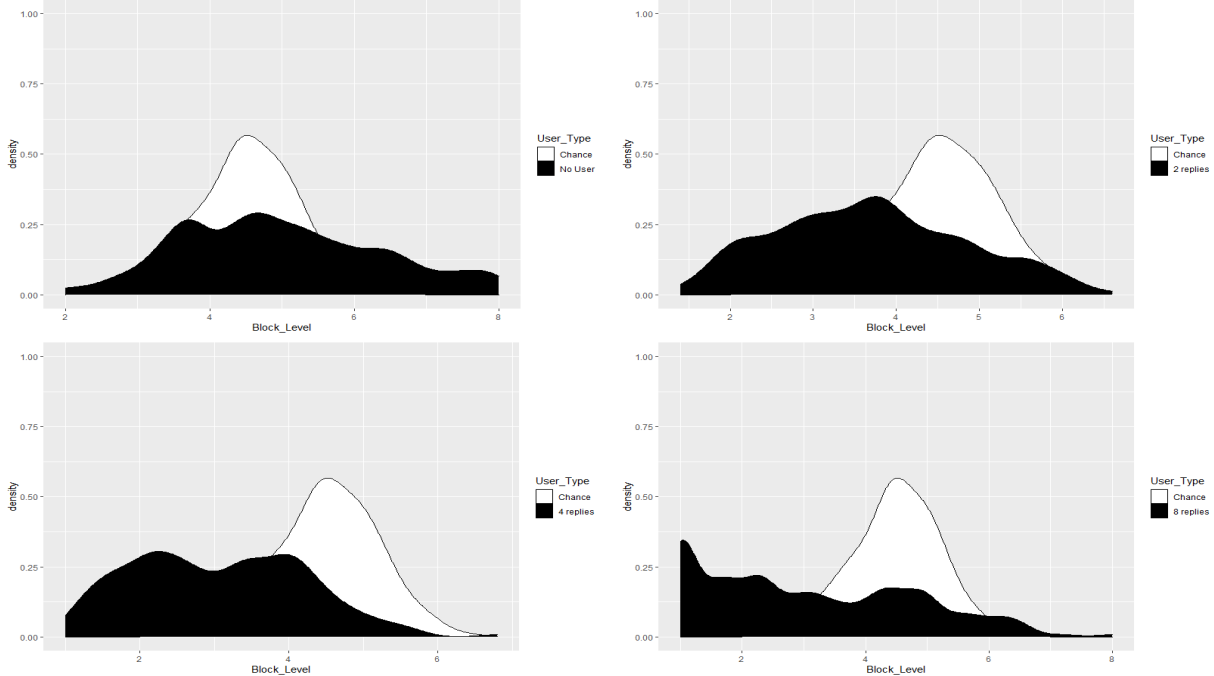


Figure 8: We consider 2000 Monte Carlo replicates of distributions as in Section 3.1.1, and from each distribution, we generate 100 networks. We use Method 2 and performance with an oracle user (varying the replies for the user; i.e., the amount of supervision provided) and the chance algorithm are compared. We plot the density of all trials (y-axis) that ranked the correct block in the n th place (x-axis).

both dissimilarity estimates provide good estimates of the the latent Δ . In the real data example considered below, there is a more pronounced differentiation across methods.

3.2 Subgraph nomination in BNU1 connectomes

Data acquisition resources and limitations can be eased through automation. For example, in the study of human connectomes, one of the more labour intensive steps, is classifying different parts of the brain. One such classification task is finding corresponding regions of interest across hemispheres in a human connectome. This task is time and human resource intensive when done manually, and automation is essential for achieving a high throughput [17]. To illustrate our HSN methodology further, we will consider then the task of nominating brain regions across hemispheres in the DT-MRI derived brain networks in the BNU1 database [43]. The spatial image of the brain includes information about its structure; in other words, the neural fibers that run through different areas of the brain. A graph of the subject’s brain is then created with the following definitions: nodes or vertices correspond to different spatial units (usually the brain is divided into cubic sections called volumetric pixels, or voxels), edges are weighted based on the amount of neural fibers that run through two regions. One may hypothesize that there is a sense of structural symmetry between paired regions across hemispheres, and discovery of this pairing is the inference task for this HSN application.

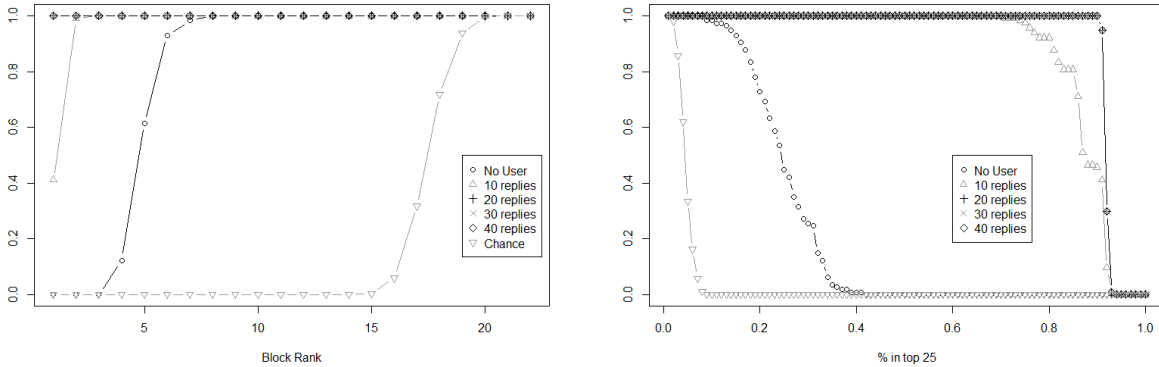


Figure 9: With perfect knowledge of the block structure of the brain (the division into 71 regions provided by the data) and using Method 1, (left) we plot on the y -axis the proportion of subjects (averaged across all blocks considered as the block-of-interest in the left hemisphere) that ranked the correct block in the right hemisphere the n -th place (x -axis); (right) we plot on the y -axis the the proportion of subjects (averaged across all blocks considered as the block-of-interest in the left hemisphere) for which we find the total proportion of the block of interest in the top 25 vertices nominated (x -axis).

Here, we apply the user aided subgraph nomination scheme to a connectomic dataset. The data we apply this to is a set of 114 neuronal networks—two repeated scans for each of 57 human subjects—derived from the BNU1 connectome dataset [43]. Each brain scan sections the brain into one thousand voxels—or volumetric pixels—with weighted edges between them indicating the amount of neuronal batches that are shared, indicating connectedness in a structural but not necessarily functional sense. Additionally each voxels contains information on it detailing its membership to the left or right hemispheres, membership to one of the 71 neuronal regions [9], whether it is grey or white matter, and its XYZ coordinates in the partially registered scan. The relative size of the networks is then ≈ 1000 vertices, with pre-defined neuronal regions varying in size between 2 and 100 vertices. As in the simulation, although the distributional properties in paired regions across hemispheres is often similar (i.e. similar motifs), there are no guarantees that the numbers of vertices that make up each region are equal. Errors from this (and misclustering) are magnified in smaller subgraphs, especially since there is less information about the motif in the small subgraph setting. The aforementioned sources of errors are mitigated by only considering paired regions that have at least 10 vertices in each hemisphere and using similarity metrics (Methods 1 and 2) that do not depend on the size of a region.

Our procedure can then be described as follows, considering each pair of sufficiently large matched regions (≥ 10 vertices in each hemisphere) separately, first we use the information given by spectrally embedding the adjacency matrix of the connectome (and the collected spatial coordinate data in Figure 11) to infer the subgraph structure in the right hemisphere via clustering by GMM [15]; using the region-of-interest in the left hemisphere as our training, next we use Methods 1 and 2 to rank above to provide different estimates of Δ . We then supply a user-in-the-loop with a vertex (or a few vertices) from each of the top k communities

to re-rank the nomination list. We plot the performance of our algorithms with perfect knowledge of the block structure of the brain (the division into 71 regions provided by the data) and using Method 1 in Figure 9. We plot:

- (Left) on the y -axis the proportion of subjects (averaged across all blocks considered as the block-of-interest in the left hemisphere) that ranked the correct block in the right hemisphere in the at worst x -th place (x -axis).
- (Right) on the y -axis the the proportion of subjects for which we find the total proportion of the block of interest in the top 25 vertices nominated (x -axis).

Note that an artifact of the metric in panel (b) is that we may never find a complete block that is of a size larger than 25 this is why we see a drop near 90%. As ideal performance in the left and right panels corresponds to the function $f(x) \equiv 1$, this figure enforces the intuition that, given high fidelity clusters, our ranking procedure is significantly better than chance and benefits strongly from user-in-the-loop supervision.

In Figure 10, in the setting of potentially errorful clusters (obtained via `Mclust` applied to the adjacency spectral embeddings of the brain networks, we plot (similar to in Figure 9), in the top panels the proportion whose match is found in the top x (similar to the left panel of Figure 10) and in the bottom panels the percent who had the proportion of the top 25 vertices come from the block of interest (similar to the right panel of Figure 10). The left two panels use Method 1 to estimate Δ , while the right two panels use Method 2. In light of perfect performance corresponding the the constant 1 function in all cases, we see here that Method 2 achieves better performance (especially for large values on the x -axis in each figure) than Method 1 both when making use of the user-supervision and in the no-user setting. Here, we see the general trend that the methods perform poorly without a user-in-the-loop (due to the error in the clustering; see Figure 11), but that the method can efficiently make use of the user to achieve better performance. As was the case previously, the clustering is errorful, and on average this can have a deleterious effect on the user-supervision (top row). However, in the bottom row we see that *sample-wise* the supervision is monotonically beneficial.

We repeat the above experiment using Method 2 and incorporating the XYZ coordinates of each voxel into the clustering (by appending the features onto the spectral graph embeddings), and plot the results in Figure 11. The increased clustering fidelity achieved by incorporating the vertex features manifests itself here by the performance gain achieved in the no-user setting when compared with Figure 10. As a result of this, better performance is achieved across all settings here (again when compared with Figure 10). While the clustering here is still errorful, and on average this can have a deleterious effect on the user-supervision, the right panel again shows that *sample-wise* the supervision is monotonically beneficial. This means that a user can successfully aid in finding larger portions of the the block of interest. Therefore, we can use these vertices in the input to further investigate and find the rest of the block, by searching in the k -nearest neighbours of these vertices.

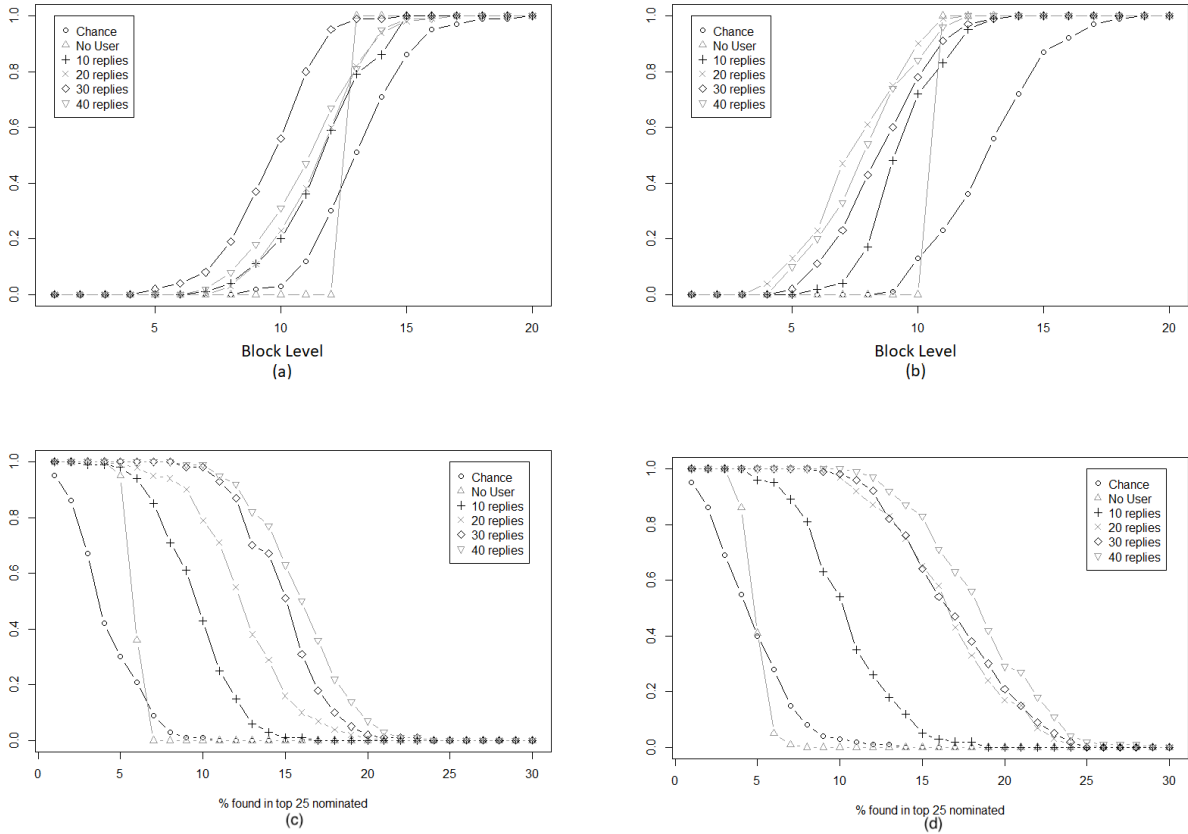


Figure 10: Clustering the graph using Gaussian Mixture Modeling on the embedded network, in the left two panels, we use Method 1 to estimate Δ , while the right two panels we use Method 2. In the top row, on the y -axis we plot the proportion of subjects (averaged across all blocks considered as the block-of-interest in the left hemisphere) that ranked the correct block in the right hemisphere the at worst x -th place (x -axis). In the bottom row, on the y -axis we plot the the proportion of subjects for which we find the total proportion of the block of interest in the top 25 vertices nominated (x -axis).

4 Conclusions and Future Direction

In this paper we have introduced a formal, and versatile framework for the novel subgraph nomination inference task, with special emphasis paid to the utility of users-in-the-loop in the context of subgraph nomination. Subgraph nomination is an important tool for structural queries within and across networks, and we demonstrated its utility in both real and synthetic data examples. In addition, the relatively simple users-in-the-loop formulation outlined herein can easily be lifted to more complex cases including supervision done over several iterations, and can be simply extended to the case of multiple users. The theory and experiments included herein highlight the important role that user supervision can play in effective information retrieval.

Further, this paper shows the importance of analysing the original algorithm and the

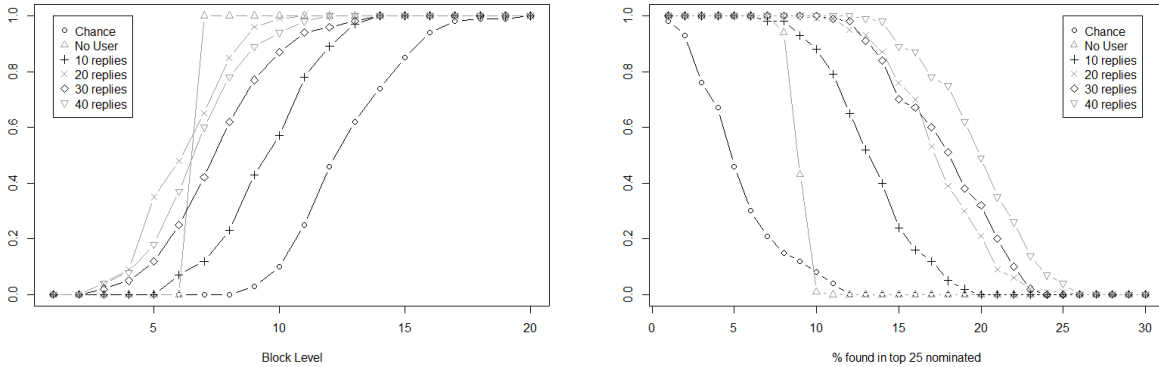


Figure 11: Clustering the embedded graphs using Gaussian Mixture Modeling incorporating the XYZ coordinate data and using Method 2 to estimate Δ . In the left panel, on the y -axis we plot the proportion of subjects (averaged across all blocks considered as the block-of-interest in the left hemisphere) that ranked the correct block in the right hemisphere the at worst x -th place (x -axis). In the right panel, on the y -axis we plot the the proportion of subjects (averaged across all blocks considered as the block-of-interest in the left hemisphere) for which we find the total proportion of the block of interest in the top 25 vertices nominated (x -axis).

validity of user input before including them. For example, if the inferred clustering is incorrect in a hierarchical subgraph nomination framework, in the sense that the correct clusters’ vertices are evenly spread among the inferred blocks, then our resources should be focused on collecting relevant data that would improve the inferred blocking structure, as even oracle user supervision in this case could be detrimental to the performance. In our approach to subgraph nomination, inferring high-fidelity clusters is essential, and we have demonstrated that clustering can be improved by incorporating informative vertex features. Exploring this further, understanding the information theoretic gain of features on our nomination performance as in [21], is an open area of research that we are actively pursuing.

The validity of the user input itself is also important to consider when thinking about adding a user-in-the-loop. While we have theoretically demonstrated the possibility of increased performance even with an errorful user, in practice the situation is significantly more nuanced. The user errors, rather than being uniformly random, may be systematic or deterministic. For example an adversarial attacks could manipulate the results of the search using a user bot attack. More nuanced users-in-the-loop demand more nuanced theory to understand their broad effects. As an example, in our nomination regime an adversary can target the obtained cluster labels for contamination. This would immediately mitigate the benefit of a user-in-the-loop, as the benefit of the user decays as the cluster fidelity worsens. More robust users would be, most likely, more costly and a cost-benefit optimization analysis would be needed in these more nuanced setting to tease out the positive (or negative) impact of incorporating the user.

Another avenue that has not been investigated explicitly but for which the framework is still sufficient is the situation with multiple blocks of interest. For that we need to adjust

the definition of the VN-user to accommodate for different values of p for each block of interest. Then, after some necessary adjustment to the loss function, one may obtain results generalized to the case of multiple blocks of interest in the simple user-in-the-loop setting. On the other hand, one may want to extend the results of Theorem 2.1 to more nuanced users.

Acknowledgement This material is based on research sponsored by the Air Force Research Laboratory and DARPA under agreement number FA8750-20-2-1001. The U.S. Government is authorized to reproduce and distribute reprints for Governmental purposes notwithstanding any copyright notation thereon. The views and conclusions contained herein are those of the authors and should not be interpreted as necessarily representing the official policies or endorsements, either expressed or implied, of the Air Force Research Laboratory and DARPA or the U.S. Government. The authors also gratefully acknowledge the support of NIH grant BRAIN U01-NS108637.

APPENDIX I: Proof of Theorem 2.1

For $i \leq j \leq c$, let the event $A_{[i,j]}$ be the event that the unknown subgraph of interest in g_2 has rank in $[i, j]$. Let E_h be the event that after user-in-the-loop supervision, the subgraph of interest has rank strictly greater than h .

Part I: With an oracle user-in-the-loop, we have that

$$\begin{aligned} \mathbb{P}(E_h) &= \underbrace{\mathbb{P}(E_h|A_{[1,h]})}_{=0} \mathbb{P}(A_{[1,h]}) + \underbrace{\mathbb{P}(E_h|A_{[h+1,h+t]})}_{=0} \mathbb{P}(A_{[h+1,h+t]}) + \underbrace{\mathbb{P}(E_h|A_{[h+t+1,m_k]})}_{=1} \mathbb{P}(A_{[h+t+1,m_k]}) \\ &= \mathbb{P}(A_{[h+t+1,m_k]}) \end{aligned}$$

If $h + t \leq c$, then $\mathbb{P}(A_{[h+t+1,k]}) = 1 - \frac{h+t}{c}$, else it is 0. Hence, $\mathbb{P}(E_h) = \max(0, 1 - \frac{h+t}{c})$ as desired.

Part II: When the user has probability p of misidentifying the vertex from the subgraph of interest as non-interesting, then when $h + t \leq c$,

$$\begin{aligned} \mathbb{P}(E_h) &= \underbrace{\mathbb{P}(E_h|A_{[1,t]})}_{=p} \mathbb{P}(A_{[1,t]}) + \underbrace{\mathbb{P}(E_h|A_{[t+1,h+t]})}_{=0} \mathbb{P}(A_{[t+1,h+t]}) + \underbrace{\mathbb{P}(E_h|A_{[h+t+1,m_k]})}_{=1} \mathbb{P}(A_{[h+t+1,m_k]}) \\ &= p\mathbb{P}(A_{[1,t]}) + \mathbb{P}(A_{[h+t+1,m_k]}) \\ &= \frac{pt}{c} + 1 - \frac{h+t}{c} = 1 - (1-p)\frac{t}{c} - \frac{h}{c}. \end{aligned}$$

When $m_k > h + t > c$, the above probability is simply $\frac{pt}{c}$.

Part III: When the user has probability p of misidentifying the vertex from the subgraph of interest as non-interesting and probability q of misidentifying a non-interesting vertex as

interesting, then when $h + t \leq c$ and $t \leq h$,

$$\begin{aligned}
\mathbb{P}(E_h) &= \underbrace{\mathbb{P}(E_h|A_{[1,t]})}_{=p} \mathbb{P}(A_{[1,t]}) + \underbrace{\mathbb{P}(E_h|A_{[t+1,h]})}_{=0} \mathbb{P}(A_{[t+1,h]}) + \sum_{i=1}^t \mathbb{P}(E_h|A_{[h+i,h+i]}) \underbrace{\mathbb{P}(A_{[h+i,h+i]})}_{=\frac{1}{c}} \\
&\quad + \underbrace{\mathbb{P}(E_h|A_{[h+t+1,m_k]})}_{=1} \mathbb{P}(A_{[h+t+1,m_k]}) \\
&= \frac{pt}{c} + \sum_{i=1}^t \frac{1}{c} \sum_{j=0}^{i-1} \binom{t}{j} (1-q)^j q^{t-j} + 1 - \frac{h+t}{c} \\
&= \frac{pt}{c} + \sum_{j=0}^{t-1} \frac{t-j}{c} \binom{t}{j} (1-q)^j q^{t-j} + 1 - \frac{h+t}{c} \\
&= \frac{pt}{c} + \sum_{j=0}^t \frac{t-j}{c} \binom{t}{j} (1-q)^j q^{t-j} + 1 - \frac{h+t}{c} \\
&= \frac{pt}{c} + \frac{qt}{c} + 1 - \frac{h+t}{c}.
\end{aligned}$$

When $h + t > c$ and $t \leq h$,

$$\begin{aligned}
\mathbb{P}(E_h) &= \underbrace{\mathbb{P}(E_h|A_{[1,t]})}_{=p} \mathbb{P}(A_{[1,t]}) + \underbrace{\mathbb{P}(E_h|A_{[t+1,h]})}_{=0} \mathbb{P}(A_{[t+1,h]}) + \sum_{i=1}^{c-h} \mathbb{P}(E_h|A_{[h+i,h+i]}) \underbrace{\mathbb{P}(A_{[h+i,h+i]})}_{=\frac{1}{c}} \\
&\quad + \underbrace{\mathbb{P}(E_h|A_{[c+1,m_k]})}_{=0} \mathbb{P}(A_{[c+1,m_k]}) + \\
&= \frac{pt}{c} + \frac{1}{c} \sum_{i=1}^{c-h} F(i-1; t, 1-q)
\end{aligned}$$

When $t > h$, and $h + t \leq c$, then

$$\begin{aligned}
\mathbb{P}(E_h) &= \underbrace{\mathbb{P}(E_h|A_{[1,h]})}_{=p} \mathbb{P}(A_{[1,h]}) + \sum_{i=1}^{t-h} \mathbb{P}(E_h|A_{[h+i,h+i]}) \underbrace{\mathbb{P}(A_{[h+i,h+i]})}_{=\frac{1}{c}} \\
&\quad + \sum_{i=t-h+1}^t \mathbb{P}(E_h|A_{[h+i,h+i]}) \underbrace{\mathbb{P}(A_{[h+i,h+i]})}_{=\frac{1}{c}} + \underbrace{\mathbb{P}(E_h|A_{[h+t+1,m_k]})}_{=1} \mathbb{P}(A_{[h+t+1,m_k]}) \\
&= \frac{ph}{c} + \sum_{i=1}^{t-h} \frac{1}{c} \left(p + (1-p) \sum_{j=0}^{i-1} \binom{h+i-1}{j} (1-q)^j q^{h+i-1-j} \right) \\
&\quad + \sum_{i=t-h+1}^t \frac{1}{c} \sum_{j=0}^{i-1} \binom{t}{j} (1-q)^j q^{t-j} + 1 - \frac{h+t}{c} \\
&= 1 - \frac{h}{c} - \frac{(1-p)t}{c} + \frac{1-p}{c} \sum_{i=1}^{t-h} F(i-1; h+i-1, 1-q) \\
&\quad + \frac{1}{c} \sum_{i=t-h+1}^t F(i-1; t, 1-q)
\end{aligned}$$

When $t > h$, and $h + t > c$, then (assuming $c \geq t, h$)

$$\begin{aligned}
\mathbb{P}(E_h) &= \underbrace{\mathbb{P}(E_h|A_{[1,h]})}_{=p} \mathbb{P}(A_{[1,h]}) + \sum_{i=1}^{t-h} \mathbb{P}(E_h|A_{[h+i,h+i]}) \underbrace{\mathbb{P}(A_{[h+i,h+i]})}_{=\frac{1}{c}} \\
&\quad + \sum_{i=t-h+1}^{c-h} \mathbb{P}(E_h|A_{[h+i,h+i]}) \underbrace{\mathbb{P}(A_{[h+i,h+i]})}_{=\frac{1}{c}} + \underbrace{\mathbb{P}(E_h|A_{[c+1,m_k]})}_{=0} \mathbb{P}(A_{[c+1,m_k]}) \\
&= \frac{pt}{c} + \frac{1-p}{c} \sum_{i=1}^{t-h} F(i-1; h+i-1, 1-q) \\
&\quad + \frac{1}{c} \sum_{i=t-h+1}^{c-h} F(i-1; t, 1-q)
\end{aligned}$$

References

- [1] J. Agterberg, Y. Park, J. Larson, C. White, C. E. Priebe, and V. Lyzinski. Vertex nomination, consistent estimation, and adversarial modification. *Electronic Journal of Statistics*, 14(2):3230–3267, 2020.
- [2] N. Alon, R. Yuster, and U. Zwick. Color-coding. *Journal of the ACM (JACM)*, 42(4):844–856, 1995.

- [3] S. Amershi, M. Cakmak, W. B. Knox, and T. Kulesza. Power to the people: The role of humans in interactive machine learning. *Ai Magazine*, 35(4):105–120, 2014.
- [4] Renzo Angles, Marcelo Arenas, Pablo Barcelo, Aidan Hogan, Juan Reutter, and Domagoj Vrgoc. Foundations of modern query languages for graph databases, 2016.
- [5] T. Caelli and S. Kosinov. An eigenspace projection clustering method for inexact graph matching. *IEEE transactions on pattern analysis and machine intelligence*, 26(4):515–519, 2004.
- [6] A. Clauset, C. Moore, and M. E. J. Newman. Hierarchical structure and the prediction of missing links in networks. *Nature*, 453:98–101, 2008.
- [7] G. Coppersmith. Vertex nomination. *Wiley Interdisciplinary Reviews: Computational Statistics*, 6(2):144–153, 2014.
- [8] L. P Cordella, P. Foggia, C. Sansone, and M. Vento. A (sub) graph isomorphism algorithm for matching large graphs. *IEEE transactions on pattern analysis and machine intelligence*, 26(10):1367–1372, 2004.
- [9] R. S. Desikan, F. Ségonne, B. Fischl, B. T. Quinn, B. C. Dickerson, D. Blacker, R. L. Buckner, A. M. Dale, R. P. Maguire, B. T. Hyman, et al. An automated labeling system for subdividing the human cerebral cortex on mri scans into gyral based regions of interest. *Neuroimage*, 31(3):968–980, 2006.
- [10] D. E. Fishkind, S. Adali, H. G. Patsolic, L. Meng, D. Singh, V. Lyzinski, and C. E. Priebe. Seeded graph matching. *Pattern recognition*, 87:203–215, 2019.
- [11] D. E. Fishkind, V. Lyzinski, H. Pao, L. Chen, and C. E. Priebe. Vertex nomination schemes for membership prediction. *The Annals of Applied Statistics*, 9(3):1510–1532, 2015.
- [12] D. E. Fishkind, V. Lyzinski, H. Pao, L. Chen, and C. E. Priebe. Vertex nomination schemes for membership prediction. *The Annals of Applied Statistics*, 9(3):1510–1532, Sep 2015.
- [13] D. E. Fishkind, L. Meng, A. Sun, C. E. Priebe, and V. Lyzinski. Alignment strength and correlation for graphs. *Pattern Recognition Letters*, 125:295–302, 2019.
- [14] C. Fraley and A. E. Raftery. Mclust: Software for model-based cluster analysis. *Journal of Classification*, 16(2):297–306, 1999.
- [15] C. Fraley and A. E. Raftery. Mclust: Software for model-based cluster analysis. *Journal of Classification*, 16(2):297–306, 1999.
- [16] B. Frénay and M. Verleysen. Classification in the presence of label noise: a survey. *IEEE transactions on neural networks and learning systems*, 25(5):845–869, 2013.

- [17] W. R. Gray, J. A. Bogovic, J. T. Vogelstein, B. A. Landman, J. L. Prince, and R. J. Vogelstein. Magnetic resonance connectome automated pipeline: an overview. *Pulse, IEEE*, 3(2):42–48, 2012.
- [18] H. S. Helm, A. Basu, A. Athreya, Y. Park, J. T. Vogelstein, M. Winding, M. Zlatic, A. Cardona, P. Bourke, J. Larson, C. White, and C. E. Priebe. Learning to rank via combining representations. *arXiv preprint arXiv:2005.10700*, 2020.
- [19] P. W. Holland, K. B. Laskey, and S. Leinhardt. Stochastic blockmodels: First steps. *Social networks*, 5(2):109–137, 1983.
- [20] H. Jin, X. He, Y. Wang, H. Li, and A. L. Bertozzi. Noisy subgraph isomorphisms on multiplex networks. In *2019 IEEE International Conference on Big Data (Big Data)*, pages 4899–4905. IEEE, 2019.
- [21] K. Levin, C. E. Priebe, and V. Lyzinski. On the role of features in vertex nomination: Content and context together are better (sometimes). *arXiv preprint arXiv:2005.02151*, 2020.
- [22] Tianxi Li, Lihua Lei, Sharmodeep Bhattacharyya, Purnamrita Sarkar, Peter J Bickel, and Elizaveta Levina. Hierarchical community detection by recursive partitioning. *arXiv preprint arXiv:1810.01509*, 2018.
- [23] T.-Y. Liu. *Learning to rank for information retrieval*. Springer Science & Business Media, 2011.
- [24] J. Lladós, E. Martí, and J. J. Villanueva. Symbol recognition by error-tolerant subgraph matching between region adjacency graphs. *IEEE Transactions on Pattern Analysis and Machine Intelligence*, 23(10):1137–1143, 2001.
- [25] V. Lyzinski, K. Levin, and C. E. Priebe. On consistent vertex nomination schemes. *Journal of Machine Learning Research*, 20(69):1–39, 2019.
- [26] V. Lyzinski, M. Tang, A. Athreya, Y. Park, and C. E. Priebe. Community detection and classification in hierarchical stochastic blockmodels. *IEEE Transactions on Network Science and Engineering*, 4(1):13–26, 2017.
- [27] D. Marchette, C. E. Priebe, and G. Coppersmith. Vertex nomination via attributed random dot product graphs. In *Proceedings of the 57th ISI World Statistics Congress*, volume 6, 2011.
- [28] R. Milo, S. Shen-Orr, S. Itzkovitz, . Kashtan, D. Chklovskii, and U. Alon. Network motifs: simple building blocks of complex networks. *Science*, 298(5594):824–827, 2002.
- [29] Jacob D. Moorman, Qinyi Chen, Thomas K. Tu, Zachary M. Boyd, and Andrea L. Bertozzi. Filtering methods for subgraph matching on multiplex networks. *2018 IEEE International Conference on Big Data (Big Data)*, 2018.

- [30] N. Natarajan, I. S. Dhillon, P. K. Ravikumar, and A. Tewari. Learning with noisy labels. In *Advances in neural information processing systems*, pages 1196–1204, 2013.
- [31] Y. Park, C. Moore, and J. S. Bader. Dynamic networks from hierarchical Bayesian graph clustering. *PLOS ONE*, 5, 2010.
- [32] H. G. Patsolic, Y. Park, V. Lyzinski, and C. E. Priebe. Vertex nomination via local neighborhood matching. *Statistical Analysis and Data Mining: The ASA Data Science Journal*, 13(3):229–244, 2020.
- [33] Tiago P. Peixoto. Hierarchical block structures and high-resolution model selection in large networks. *Physical Review X*, 4(011047):1–18, 2014.
- [34] P. Rastogi, V. Lyzinski, and B. Van Durme. Vertex nomination on the cold start knowledge graph. *Human Language Technology Center of Excellence: Technical report*, 2017.
- [35] P. Rastogi, A. Poliak, V. Lyzinski, and B. Van Durme. Neural variational entity set expansion for automatically populated knowledge graphs. *Information Retrieval Journal*, 22(3-4):232–255, 2019.
- [36] M. Sales-Pardo, R. Guimerà, A. A. Moreira, and L. A. N. Amaral. Extracting the hierarchical organization of complex systems. *Proc. Natl. Acad. Sci. U.S.A.*, 104, 2007.
- [37] G. M Slota and K. Madduri. Fast approximate subgraph counting and enumeration. In *2013 42nd International Conference on Parallel Processing*, pages 210–219. IEEE, 2013.
- [38] D. L. Sussman, V. Lyzinski, Y. Park, and C. E. Priebe. Matched filters for noisy induced subgraph detection. *IEEE Transactions on Pattern Analysis and Machine Intelligence*, 2019.
- [39] S. Suwan, D. S. Lee, and C. E. Priebe. Bayesian vertex nomination using content and context. *Wiley Interdisciplinary Reviews: Computational Statistics*, 7(6):400–416, 2015.
- [40] M. Tang, A. Athreya, D. L. Sussman, V. Lyzinski, and C. E. Priebe. A nonparametric two-sample hypothesis testing for random dot product graphs. *Bernoulli*, 23:1599–1630, 2017.
- [41] J. R. Ullmann. An algorithm for subgraph isomorphism. *Journal of the ACM (JACM)*, 23(1):31–42, 1976.
- [42] J. Yoder, L. Chen, H. Pao, E. Bridgeford, K. Levin, D. E. Fishkind, C. E. Priebe, and V. Lyzinski. Vertex nomination: The canonical sampling and the extended spectral nomination schemes. *Computational Statistics & Data Analysis*, 145:106916, 2020.
- [43] X.-N. Zuo, J. S. Anderson, P. Bellec, R. M. Birn, B. B. Biswal, J. Blautzik, J. C. S. Breitner, R. L. Buckner, V. D. Calhoun, F. X. Castellanos, et al. An open science resource for establishing reliability and reproducibility in functional connectomics. *Scientific data*, 1(1):1–13, 2014.